The phase lag in three fourier frequency ranges of black hole transients

Reporter: Xiao Guangcheng
Mentor: Qu Jinlu
Institute of High Energy Physics

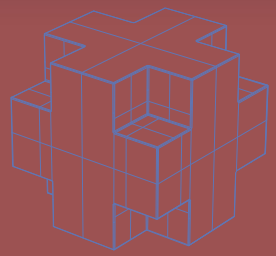

Email: xiaogc@ihep.ac.cn

MAIN CONTENTS

- Introduction to black-hole transients
- QPO and time lag models
- Research method
  - Coherence function， Phase lag
  - Three frequency ranges： Band-limited noise， Red noise and QPO
- The case of XTE J1650-500
  - Results
  - Discussion
- Preliminary results of other transients
  - Results and possible classification
  - Discussion

• An brief introduction to black hole transients

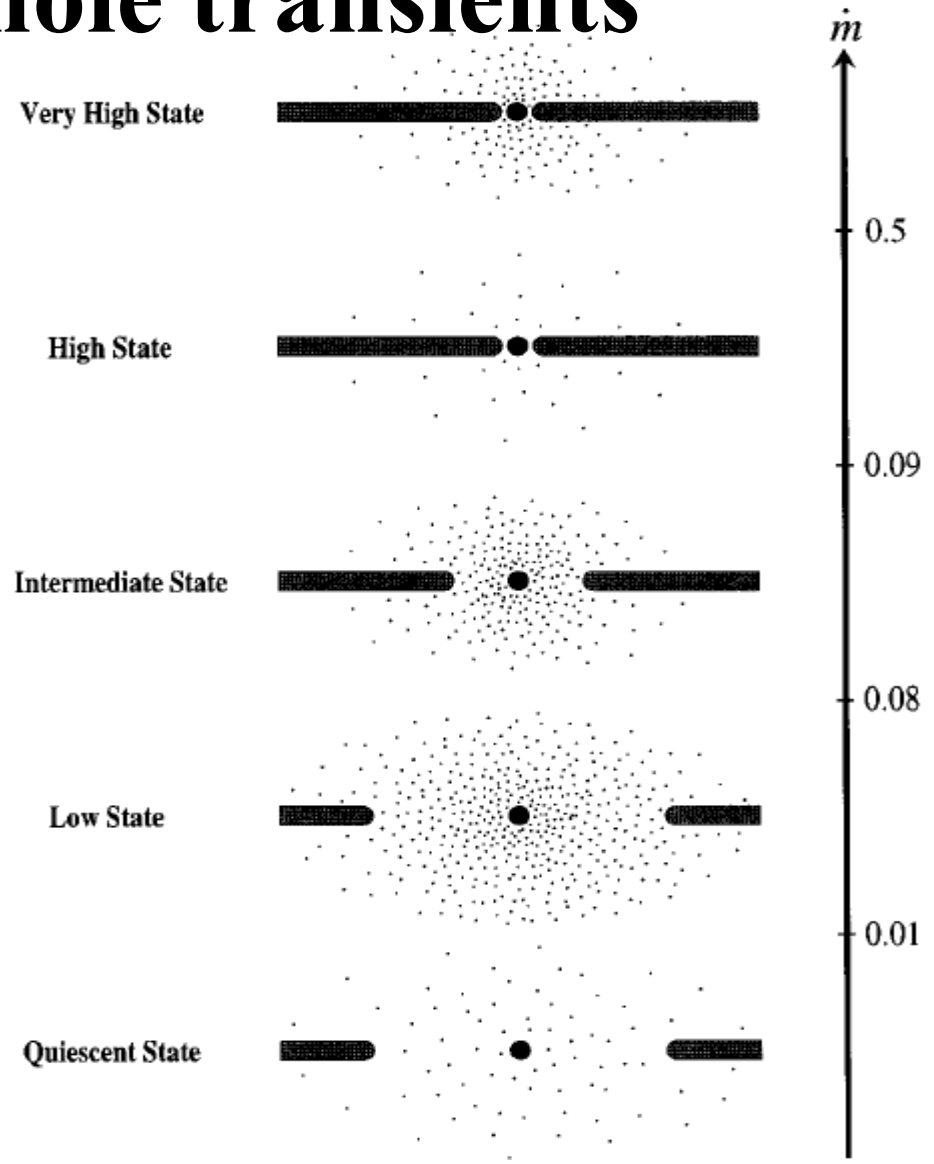

A full outburst may contains:
QS→LHS→HIMS →SIMS→TD→SI MS→HIMS→LHS →QS

FIG. 1.—Configuration of the accretion flow in different spectral states shown schematically as a function of the total mass accretion rate $\dot{m}$. The ADAF is indicated by dots and the thin disk by the horizontal bars. The lowest horizontal panel shows the quiescent state, which corresponds to a low-mass accretion rate (and therefore, a low ADAF density) and a large transition radius. The next panel shows the low state, where the mass accretion rate is larger than in the quiescent state, but still below the critical value $\dot{m}_{\rm crit} \sim 0.08$. In the intermediate state (*middle panel*), $\dot{m} \gtrsim \dot{m}_{\rm crit}$ and the transition radius is smaller than in the quiescent/low state. In the high state, the thin disk extends down to the last stable orbit and the ADAF is confined to a low-density corona above the thin disk. Finally, in the very high state, we make the tentative proposal that the corona has a substantially larger $\dot{m}$ than in the high state.

• The related black-hole transients

Inclination	transients	Outburst year	QPO (Hz)	Comments
Type-C Low Inclination	Swift J1753.5-0127	05, 10	0.37-0.90	Include failed burst
	4U 1543-47	02	4.3-11	Low Q factor
	XTE J1650-500	01	1.3-6.8	
	GX 339-4	02, 04, 07, 10	0.2-12	Obvious harmonic
	XTE J1752-223	09	2.2-6.4	
	XTE J1818-330	06	10-11	
Type-C Middle Inclination	XTE J1859+226	99	1.2-7.6	QPO soft time lag
	MAXI J1543-564	11	1.0-5.7	
Type-C High Inclination	XTE J1550-564	98, 00	0.1-13	Obvious harmonic
	4U 1630-47	02-04, 05	0.79-14.8	Low Q factor
	GRO J1655-40	96, 05	0.1-21	
	H 1743-322	03, 04, 08, 09, 10	0.11-9.44	Obvious harmonic
	MAXI J1659-152	10	1.6-7.3	
	XTE J1748-288	98	17-31	Relatively high f_{QPO}

• QPO and Time lag models

Time lag models

- Static Compton Cloud Models
- The Dynamic Compton Cloud
- Small Scale Spectral Transitions
- Reverberation

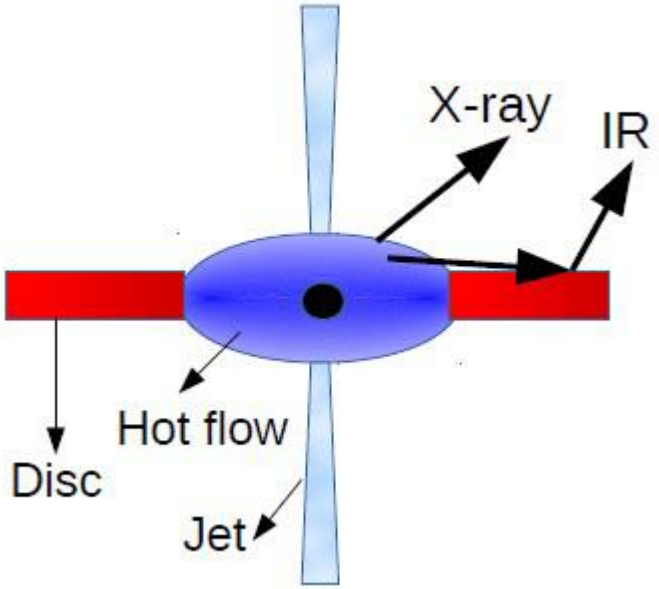

QPO models

- Magneto-acoustic Wave Propagation Model
- Lense-Thirring Precession

Figure 2. Schematic diagram of the geometry considered. The inner flow (grey with blue angular momentum vector) precesses about the black hole angular momentum vector whilst the outer disc (red/orange) remains aligned with the binary partner. The flow extends between r_i and r_o.

• Research method

- Coherence function： to calculate the correlation of two concurrent time series in the fourier frequency domain.

$$\gamma^2(f) = \frac{|\langle S^*(f)H(f)\rangle|}{\langle |S(f)|^2\rangle\langle |H(f)|^2\rangle}$$

1 for totally correlated， 0 for totally uncorrelated

- Phase lag： $\phi(f) = \arg[C(f)]$， in which

$$C(f) = \langle S^*(f)H(f)\rangle$$

- Time lag： $\tau(f) = \phi/2\pi f$

- Study the PDS， Coherence and phase lag features and evolution during outburst. The timing parameters are **averaged** in three fourier frequency range： band-limited noise(0.03-0.8 Hz)， red noise(1-10 Hz) and QPOs.

- **In the case of XTE J1650-500**

Introduction of XTE J1650-500

☐ Binary system information

- Found in 2001 outburst
- companion star mass function $2.73 \pm 0.56\ M_{\odot}$, orbital inclination $50° \pm 3°$, the upper limit mass of compact star $\sim 7.3\ M_{\odot}$

☐ Substantial outburst features

- High frequency QPO (~64 HZ)
- Relativistically broadened iron emission lines
- Short time scale X-ray flare (~100 s)
- Radio observation and jets

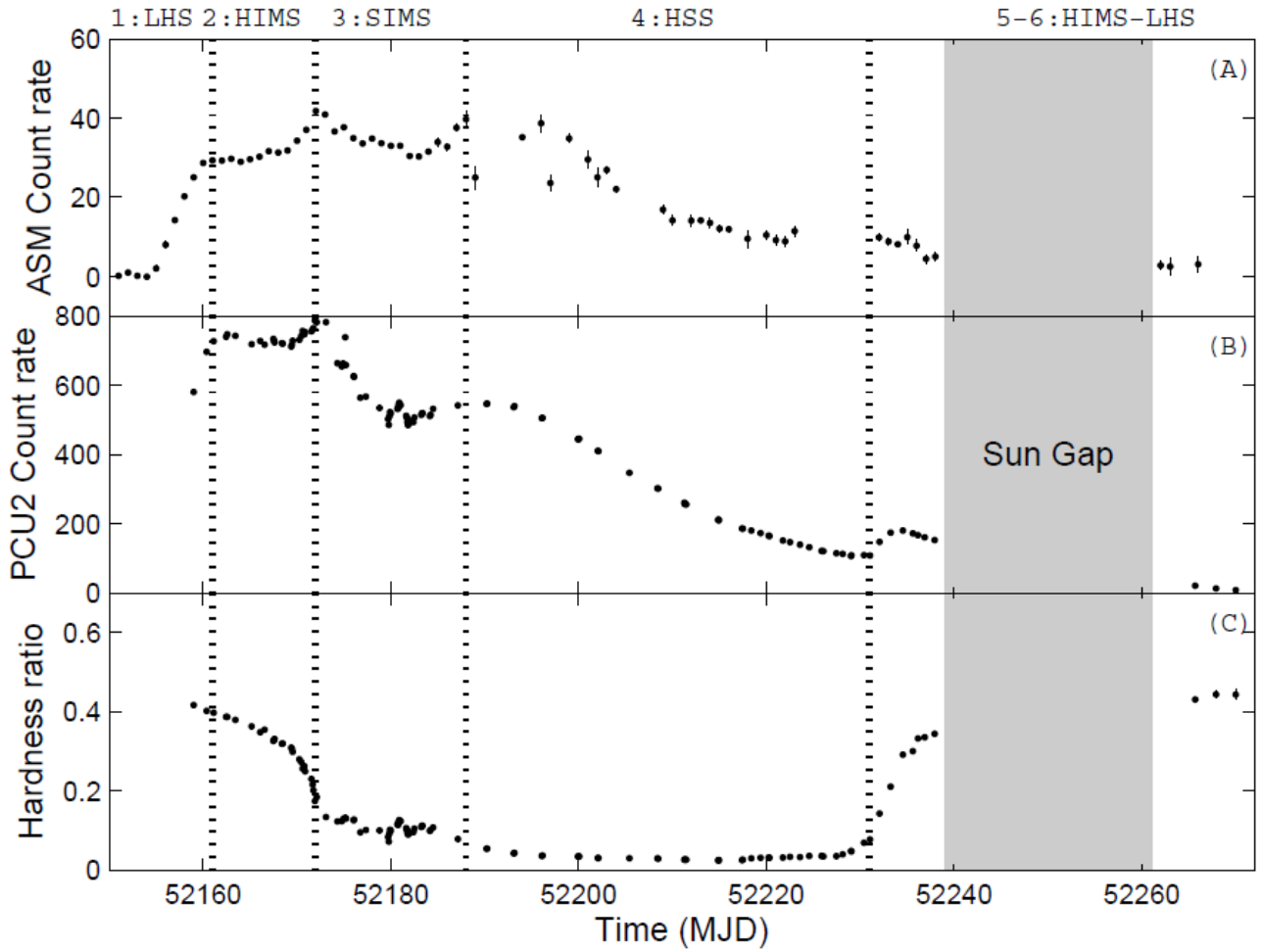

Fig. 1 Light curves and hardness evolution diagram. Panel A: light curve from PCA/ASM detector with time resolution of one day. Panel B: light curve from RXTE/PCU2, each point corresponding to one observation. Panel C: hardness evolution diagram whose hardness is the ratio between 6.3-8.4 keV and 2.1-5.8 keV photon flux. The outburst of the transient show 4 states namely low-hard state(LHS), hard intermediate state(HIMS), soft intermediate state(SIMS) and high-soft state(HSS). QPOs mainly show in HIMS. The observation was paused for the sake of protecting the satellite from the sun.

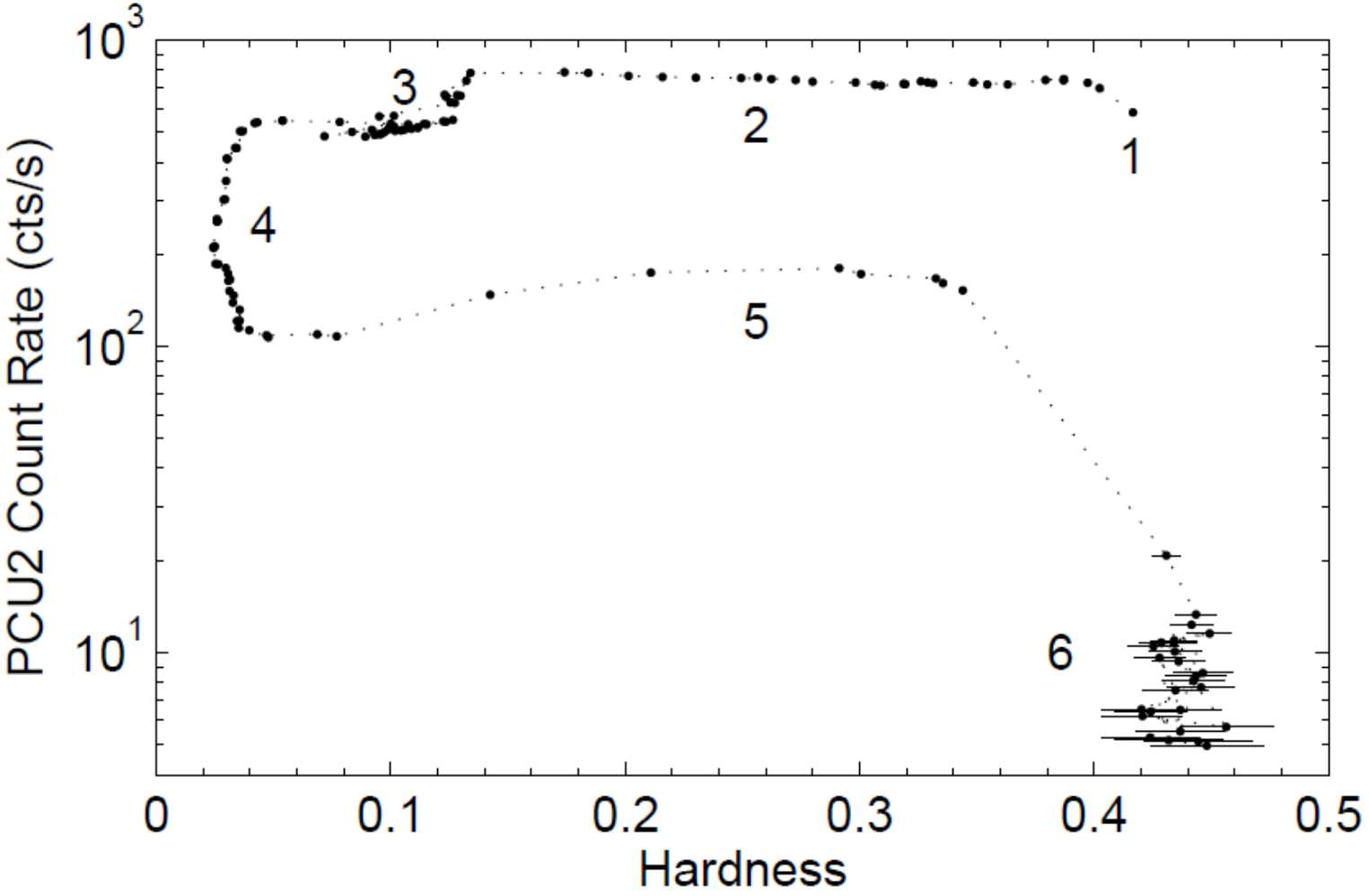

Fig. 2 Hardness-intensity diagram. Hardness calculation method is the same as fig 1 and the intensity is the photon count rate in 2.1-8.4 keV energy band. The accretion states can be distinguished from the HID.

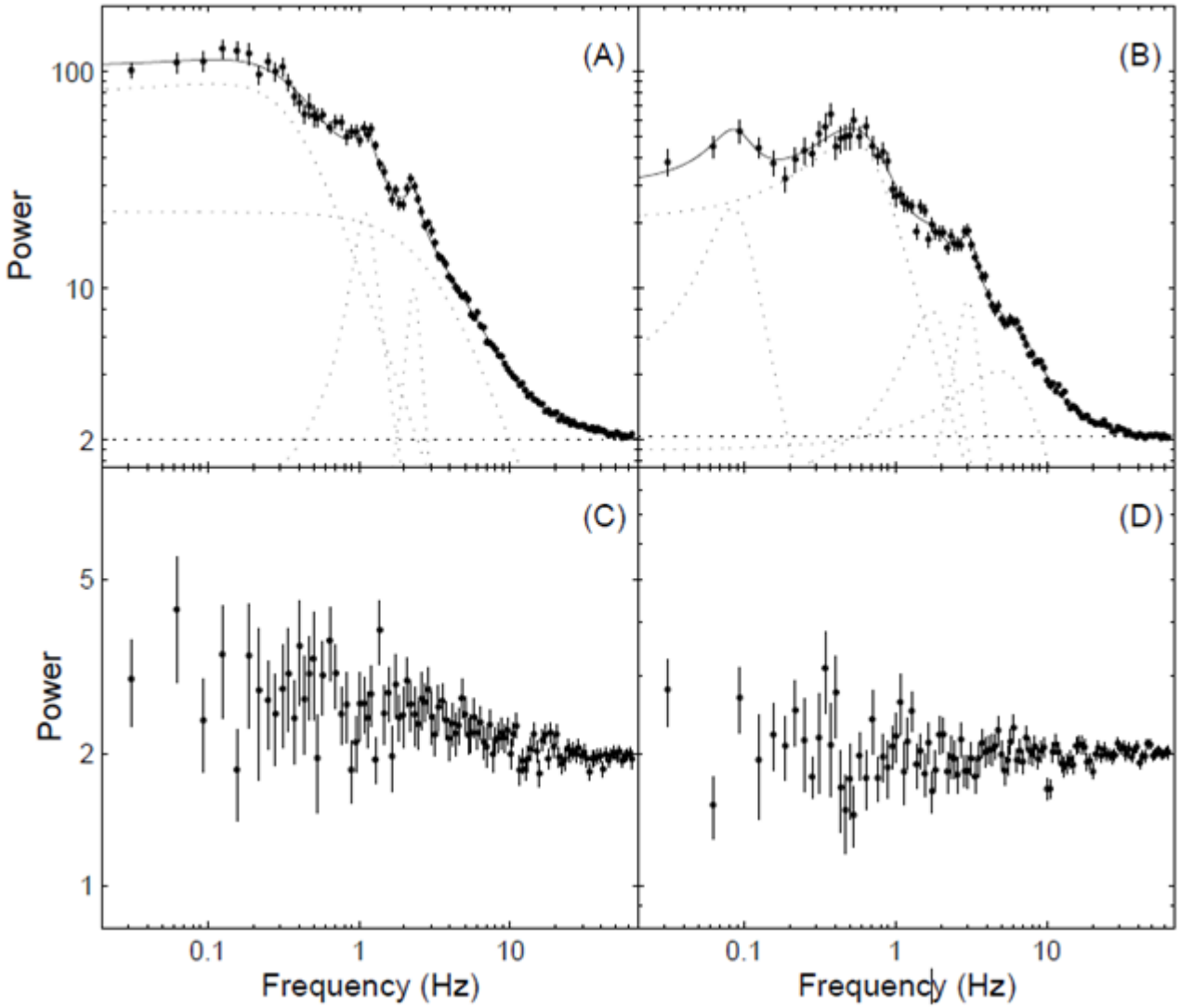

Fig. 3 Typical PDSs from each accretion state. Four panels correspond to LHS, HIMS, SIMS, HHS respectively, and the matching observation IDs are 60113-01-04-00, 60113-01-10-01, 60113-01-19-06, 60113-01-33-00.

Band-limited noise: 0.03-0.8 Hz

Red noise: 1-10 Hz

QPO freqency range

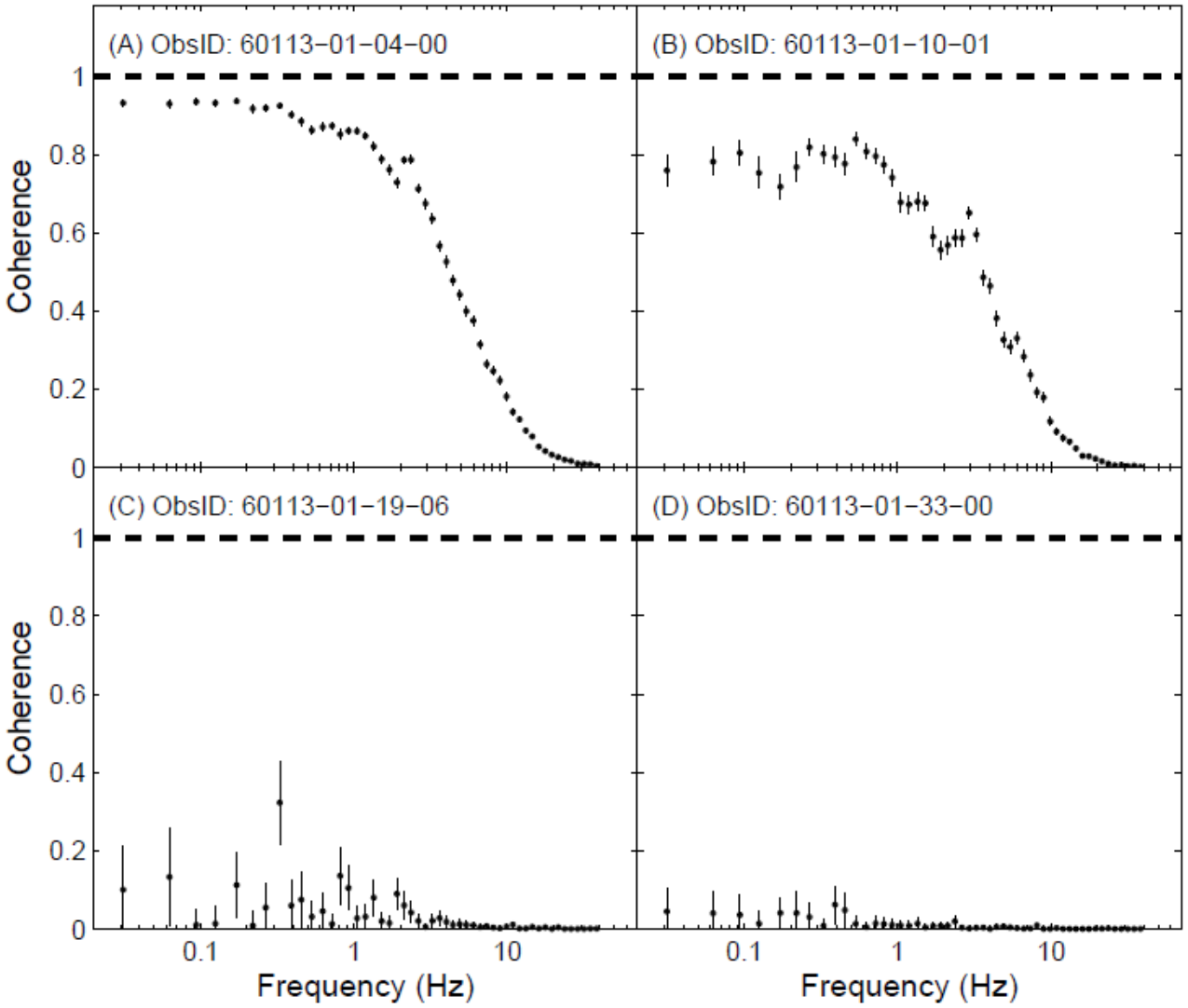

图 4　暂现源在各谱态下的相干函数. A、B、C、D依次为低硬态、硬中间态、软中间态和高软态, 每个态都取一次观测作为代表示例. 随着暂现源向高软态演化, 各个频率段的相关系数降低.

Fig. 4　Typical coherence function for each accretion state. The same observations are selected as in fig 3. With the energy spectrum getting softer, the coherence coefficient gets lower in each frequency range.

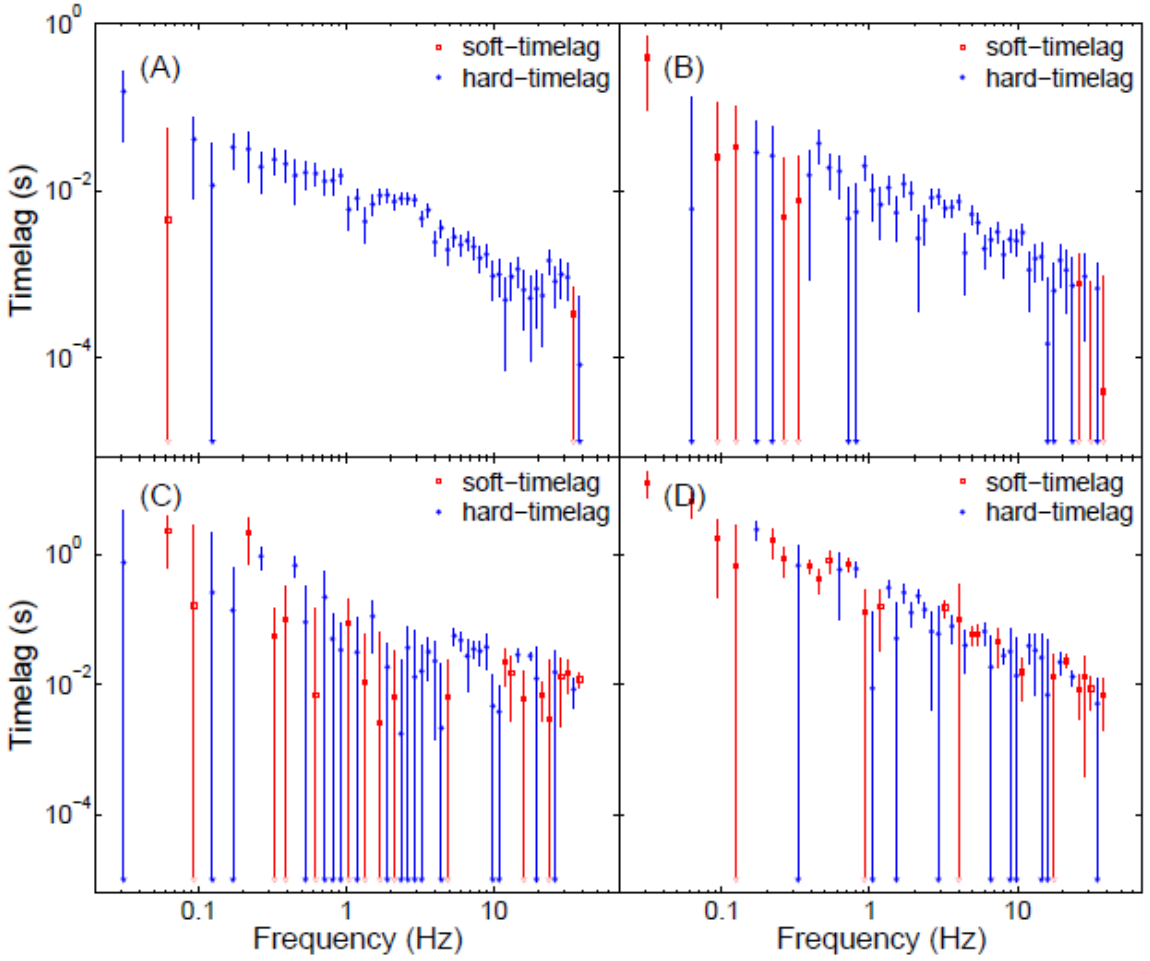

图 5　暂现源在各态下的时间延迟谱. 各子图对应的观测号及光变曲线能道的选择与图4 一致.

Fig. 5　Typical f-timelag spectrum for each accretion state. The observation IDs and energy bands are the same as the PDS and coherence function analysis.

For XTE J1650-500, the dependence of time lag on frequency varies with accretion states. Similarly to the $\tau(f) \propto f^{-0.7}$ presented in Cyg X-1,fitting fig A gives $\tau(f) \propto f^{-0.86\pm0.12}$ with 95% confidence.

- **Results in Band-limited noise freq. range**

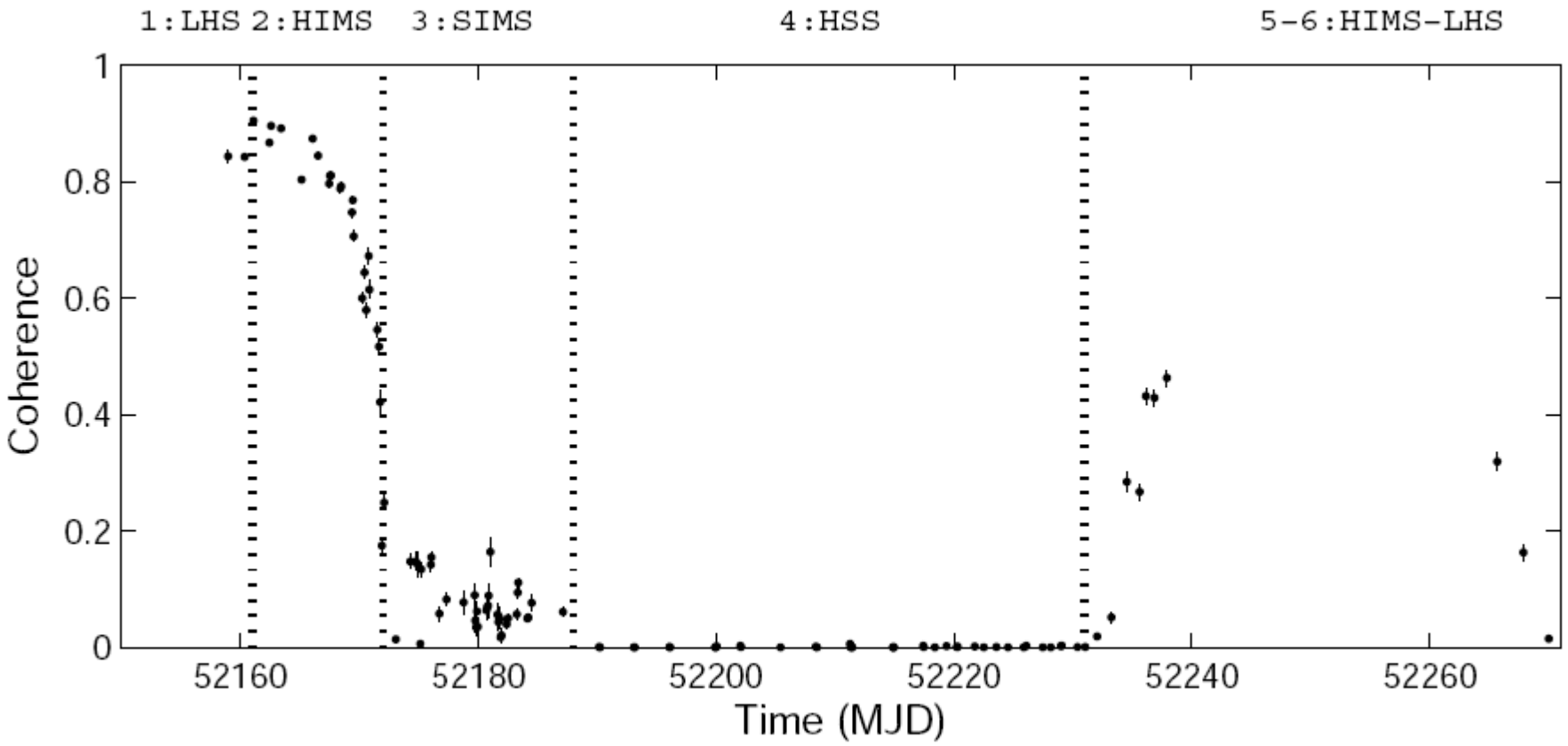

图 6　宽限噪声频段(0.03-0.8 Hz）相干系数的演化图.

Fig. 6　The coherence coefficient evolution diagram in the frequency range of band limited noise(0.03-0.8 Hz).

- **Results in Band-limited noise freq. range**

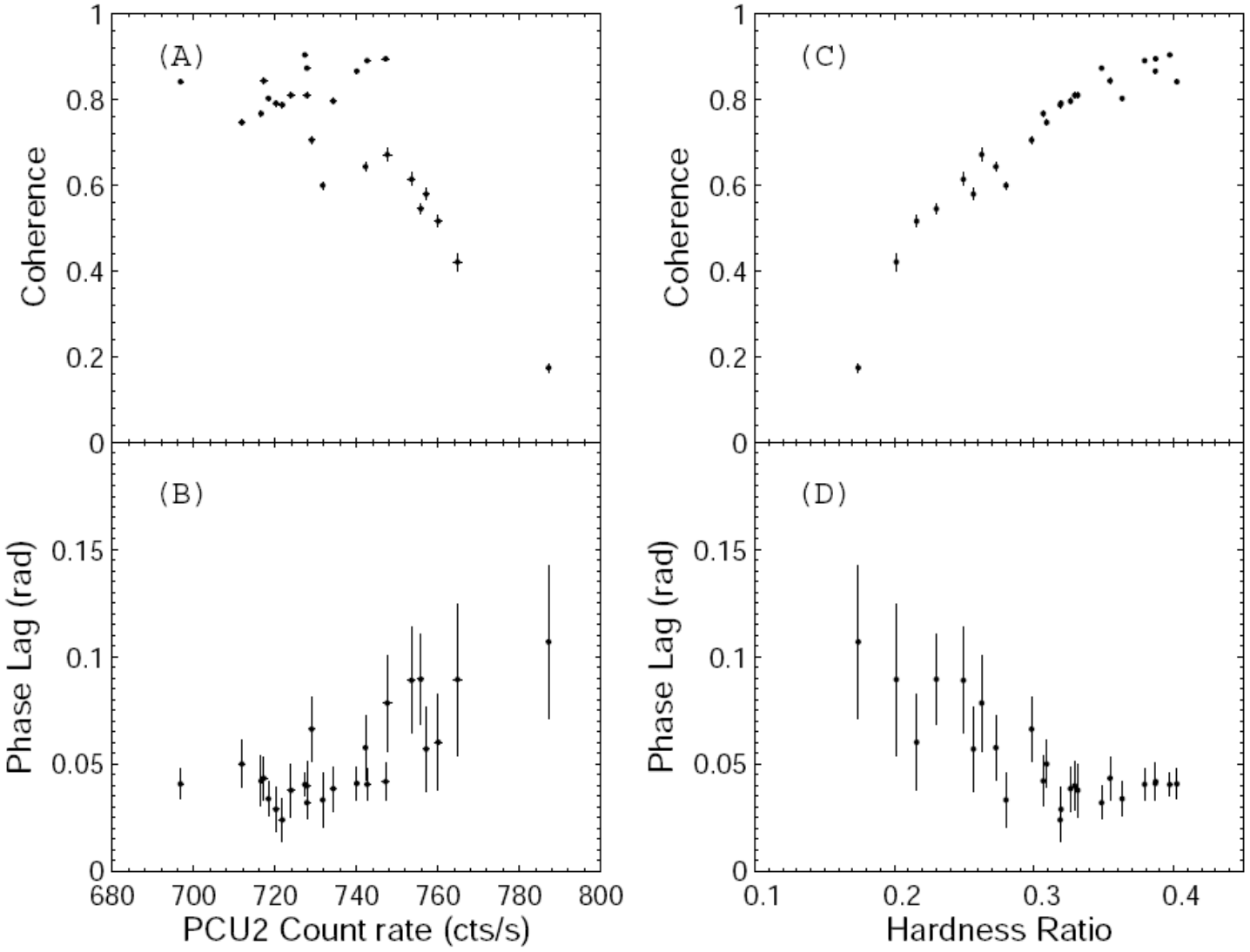

图 7　低硬态与硬中间态下的宽限噪声频段的平均相干函数、相位延迟随暂现源流强、硬度的变化图.

- **Results in red noise freq. range**

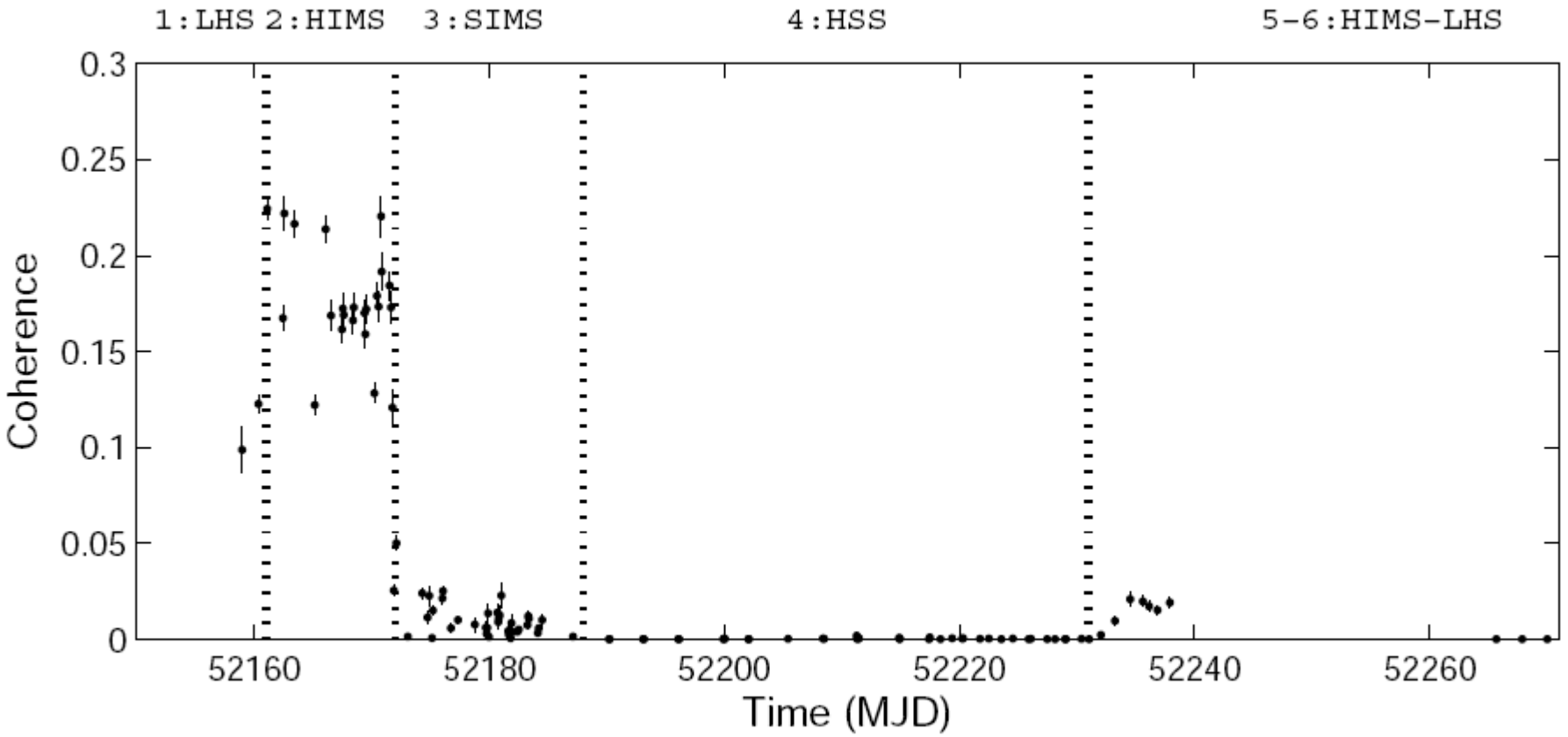

图 8　红噪声频率范围(7.5-10 Hz）相干系数演化图.

Fig. 8　The coherence coefficient evolution diagram in the frequency range of red noise(7.5-10 Hz)

- **Results in red noise freq. range**

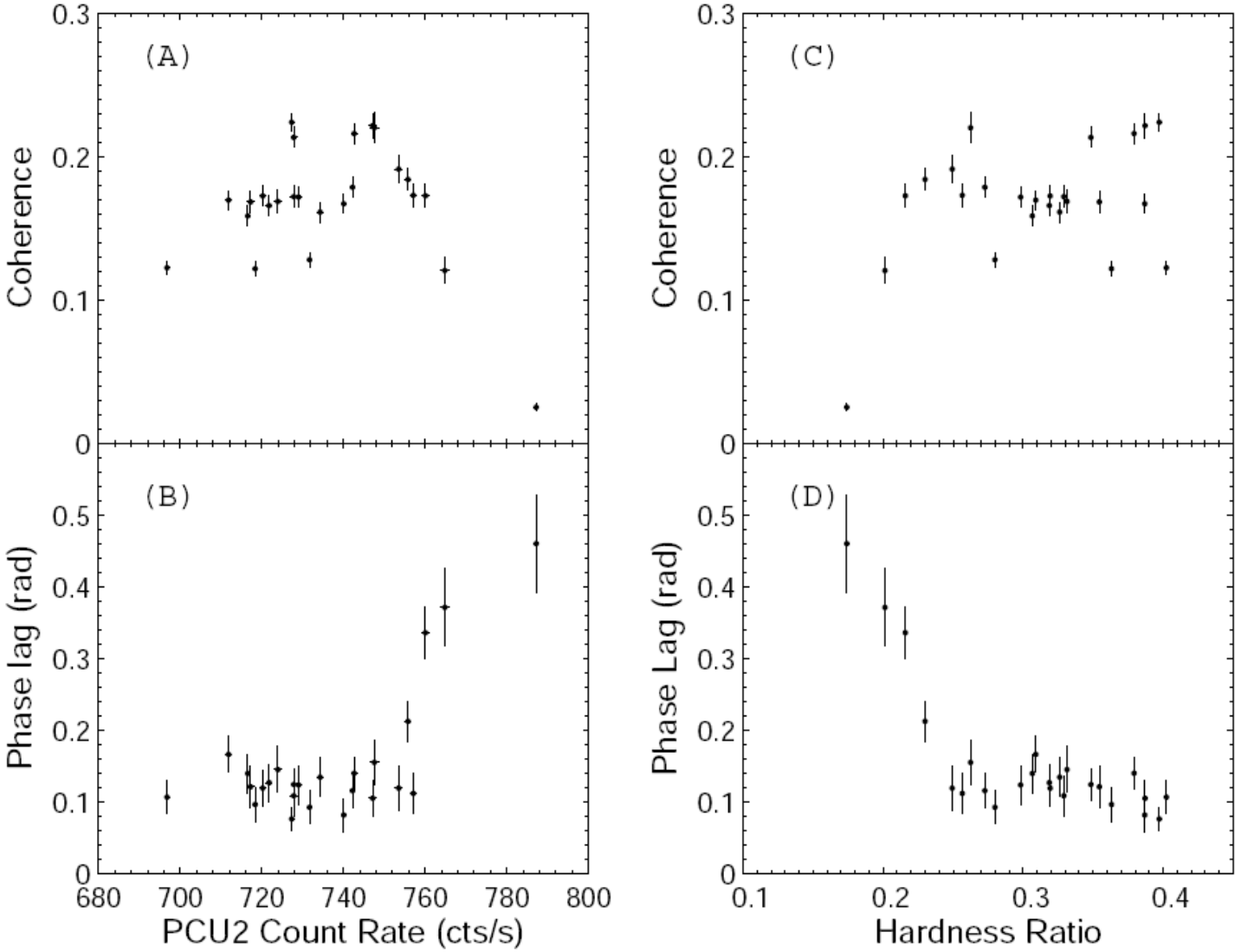

图 9　低硬态与硬中间态下的红噪声频率范围(7.5-10）相干系数、相位延迟随随暂现源流强、硬度的变化图. 光变曲线能道选取与宽限噪声处做法相同.

- **Results in QPO noise freq. range**

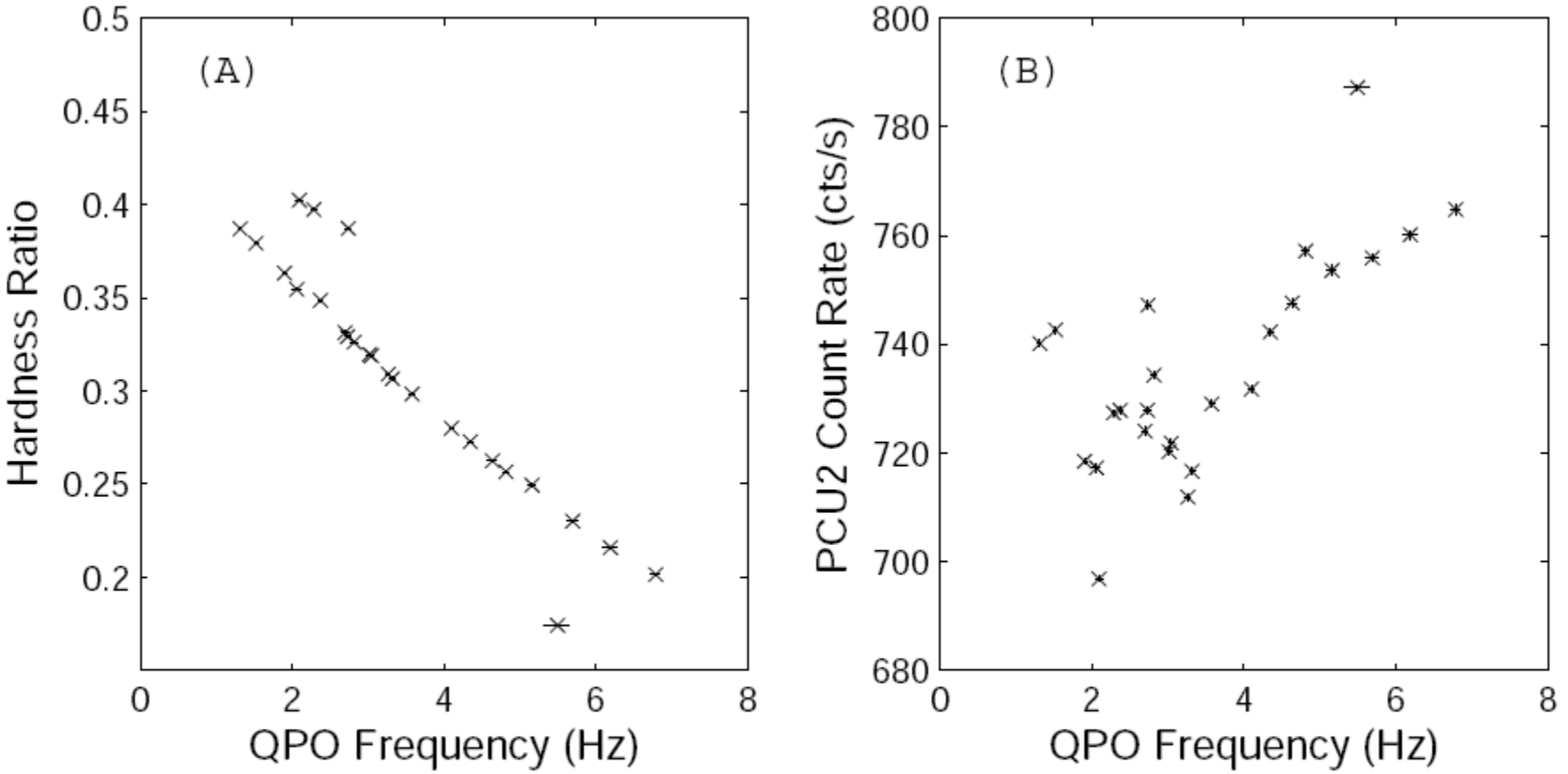

图 10　红噪声频率范围(7.5-10 Hz)相干系数演化图.

Fig. 10　The coherence coefficient evolution diagram in the frequency range of QPOs

- **Results in QPO noise freq. range**

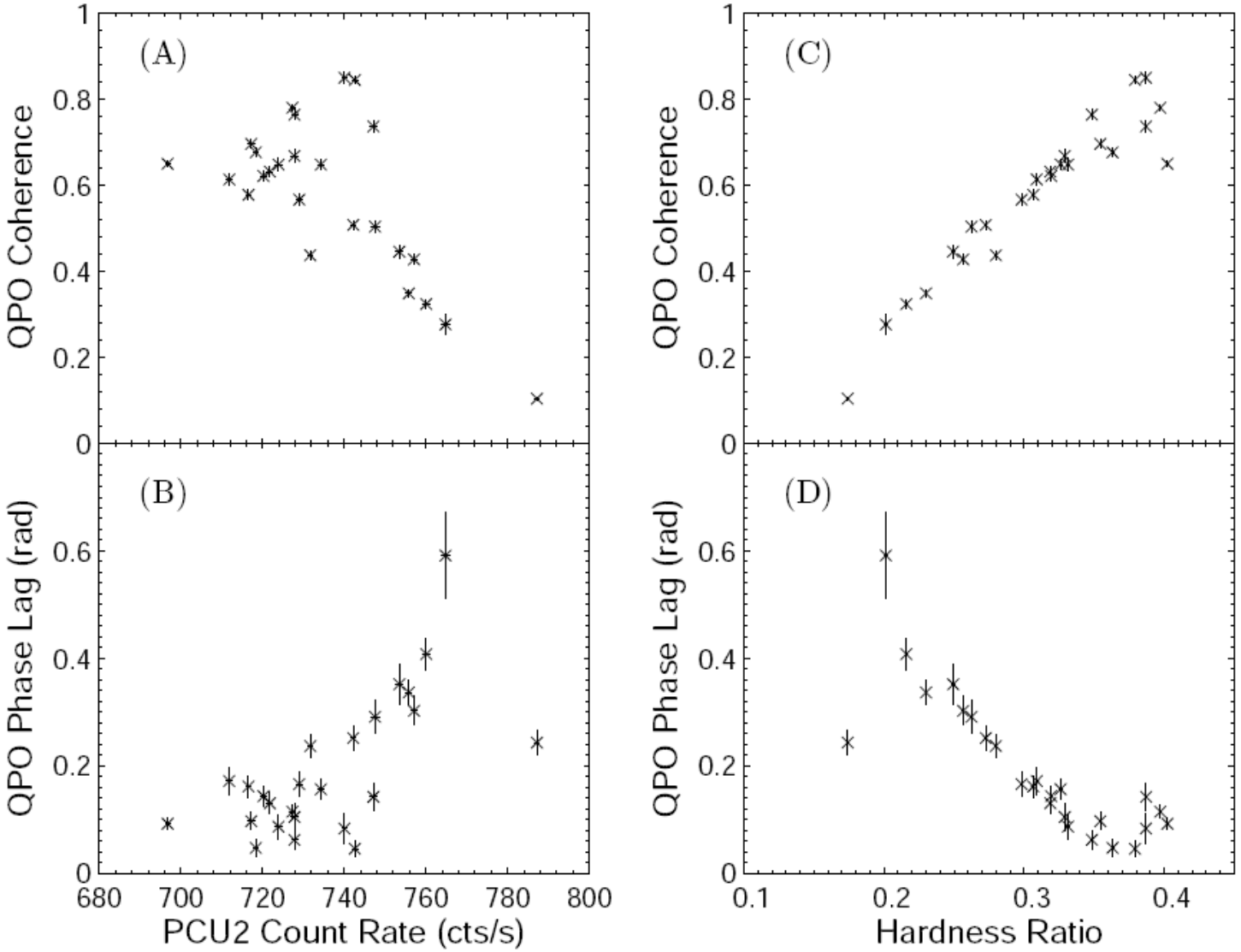

图 11　QPO频率范围内的相干系数、相位延迟随暂现源流强、硬度的变化图.

- **Results in QPO noise freq. range**

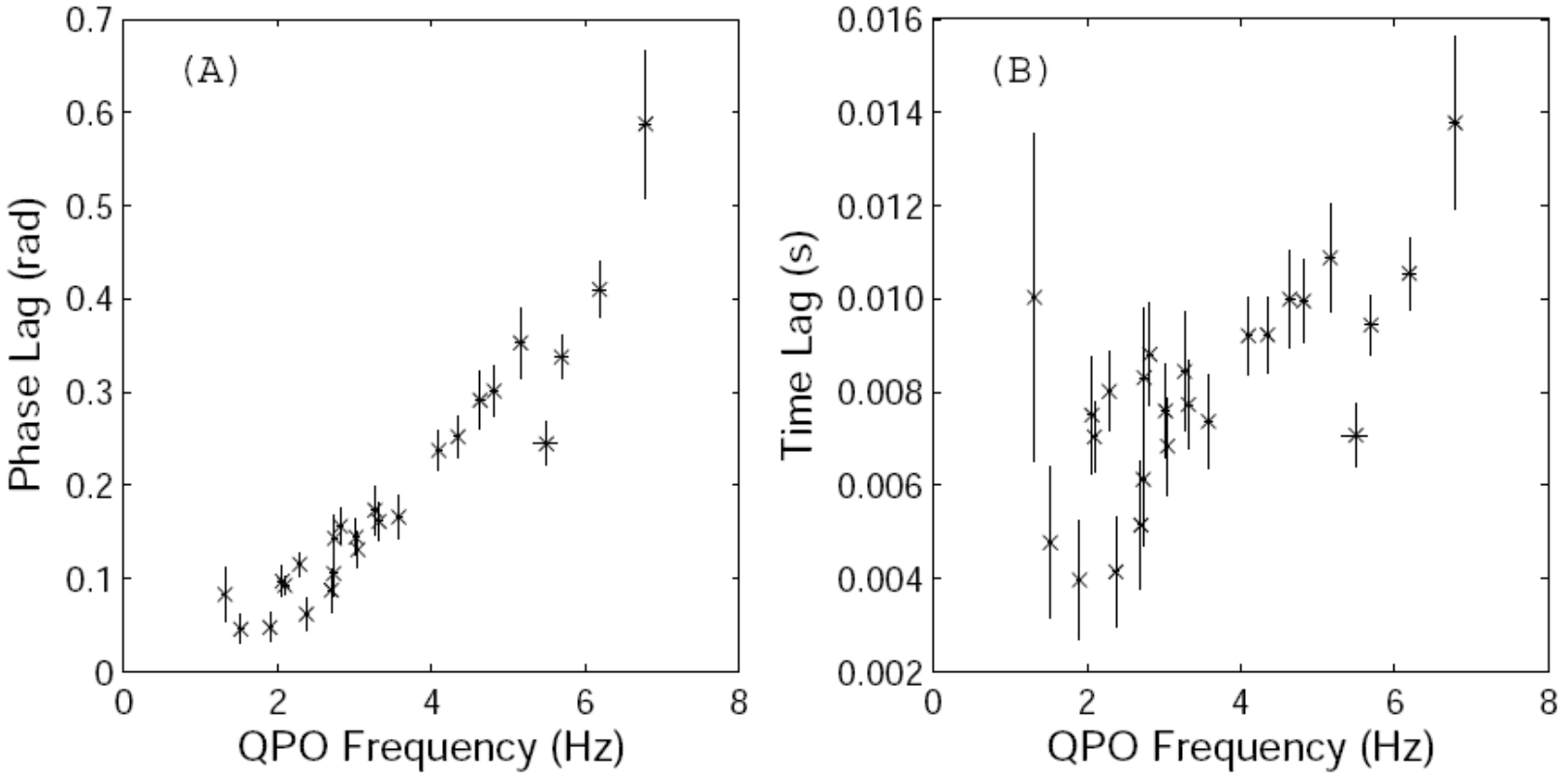

图 12　QPO频率范围的相位延迟与时间延迟分别随QPO中心频率的变化图.

Fig. 12　The mean phase lag and timelag in the QPOs frequency range as the function of the central frequency of QPOs

- **Brief summary and discussion**

Our findings (mainly for LHS/HIMS)

- **Time lag dependent on frequency**
- **In BLN freq. range**
  - $(Flux\nearrow, \gamma^2\swarrow)$, (Hard ratio $\swarrow, \gamma^2\nearrow$)
  - $(Flux\nearrow, \phi_{\rm BLN}\nearrow)$, (Hard ratio $\swarrow, \phi_{\rm BLN}\nearrow$)
- **In red noise freq. range**
  - $\phi_{\rm BLN}$, γ^2 trend to stay **constant**, while a **breakpoint** may exit and more obvious.
- **In QPO freq. range**
  - $(Flux\nearrow, f_{QPO}\nearrow)$, (Hard ratio $\swarrow, f_{QPO}\nearrow$)
  - The dependence of γ^2 and $\phi_{\rm QPO}$ on flux and hard ratio is similar to that of BLN.
  - $(f_{QPO}\nearrow, \phi_{\rm QPO}\nearrow,)$, $(f_{QPO}\nearrow, \tau_{QPO}\nearrow)$

• Conclusions

- $\tau(f) \propto f^{-0.86\pm0.12}, hard\ delay.$
  - x Static Compton Cloud Models
  - ✓ Fluctuation Propagation
  - ? Pure reverberatio
- Results from QPO freq. range
  - ✓ Fluctuation Propagation in 'truncated disk' geometry

$$C_s = \sqrt{\frac{kT_0}{m_p}} \approx 3.1 \times 10^8 \left(\frac{T_0}{100keV}\right)^{\frac{1}{2}} cm\, s^{-1} \qquad (4.1)$$

- Time lag can't be explained within single mechanism
  - 'Fluctuation Propagation + Reverberation' model

- Preliminary results of other transients (QPO)

➢ Swift J1753.5-0127

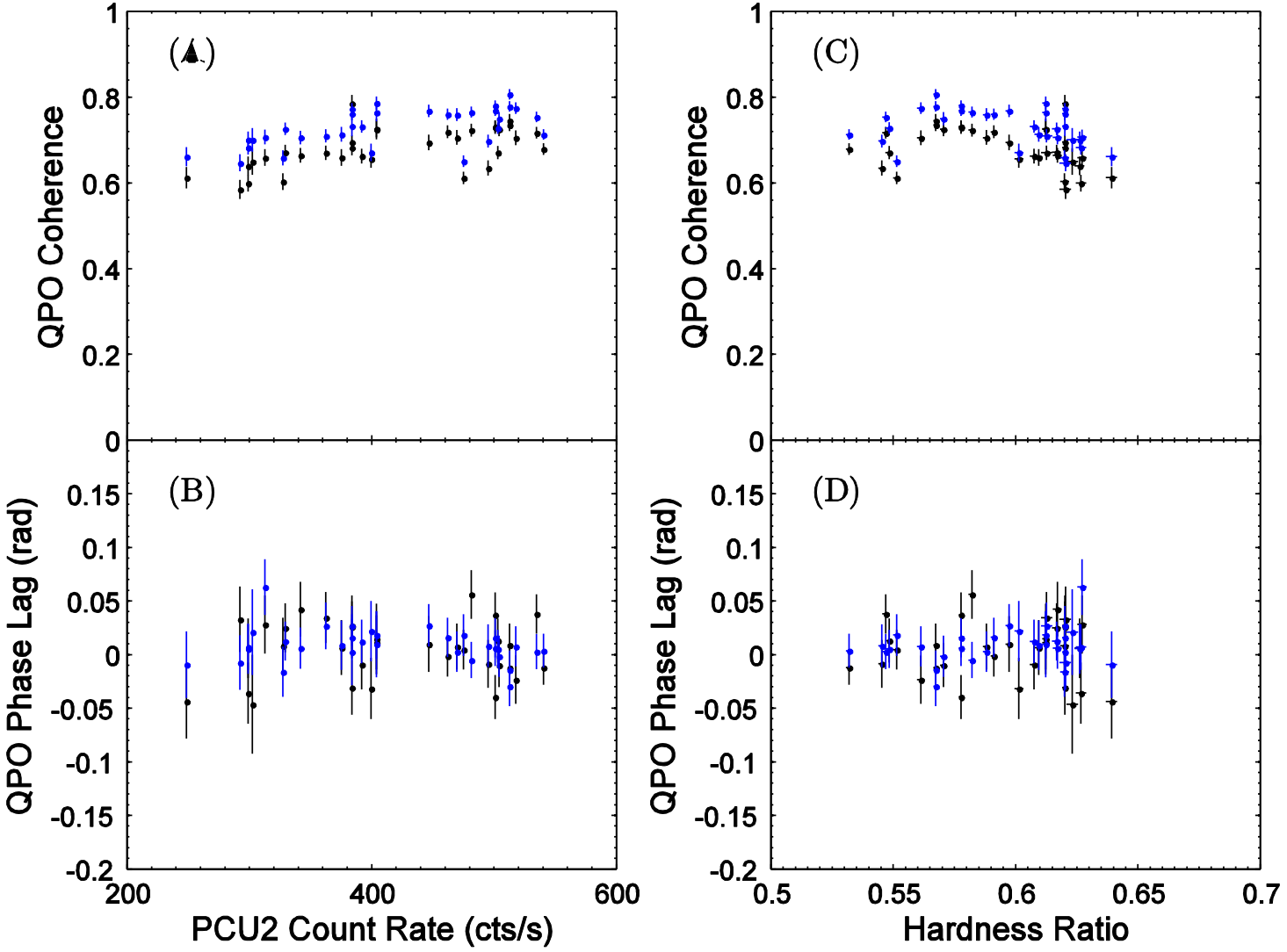

Swift J1753.5-0127

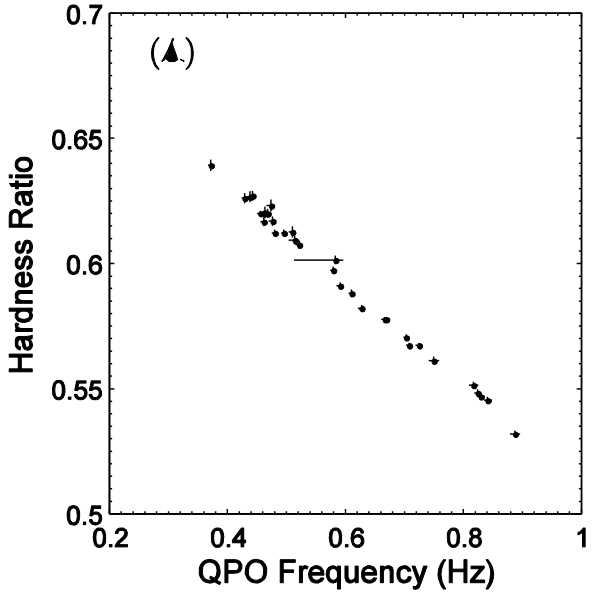

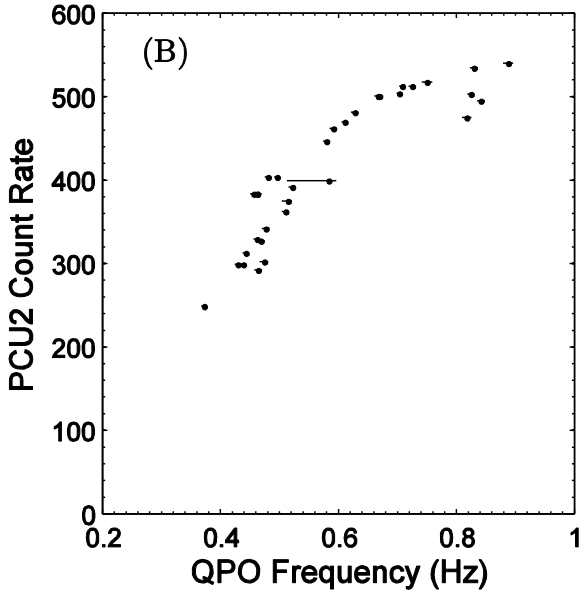

Flux and Hardness ratio are well correlated with QPO central Frequency.

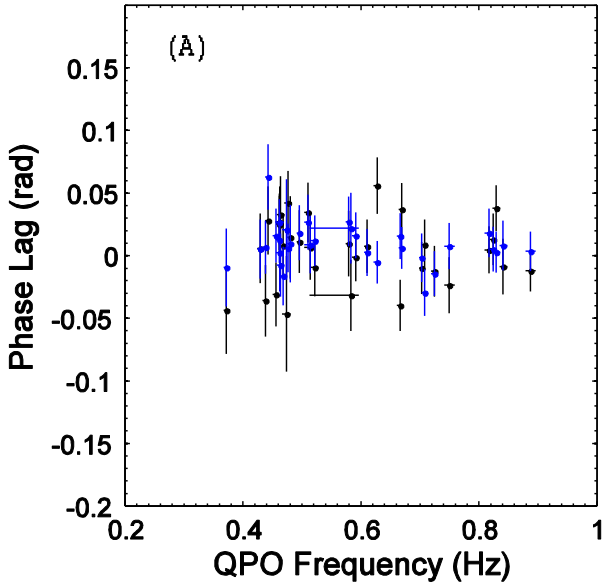

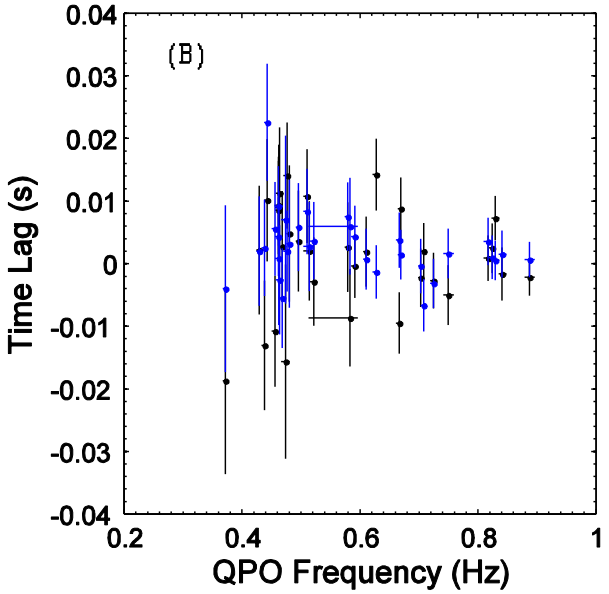

Time lag stay close to zero despite the evolution of QPO central Frequency.

XTE J1859+226 (Soft Delay)

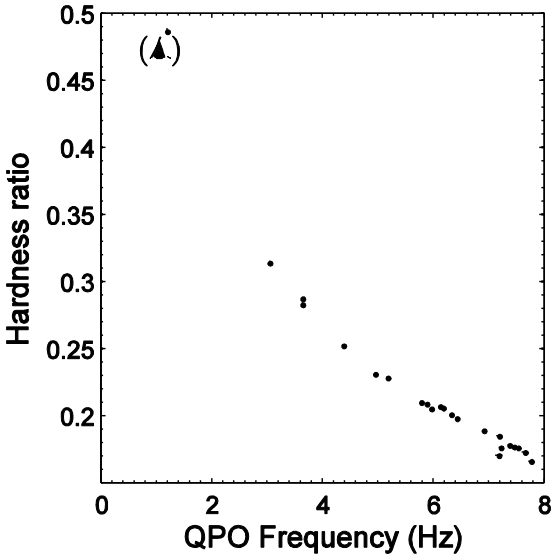

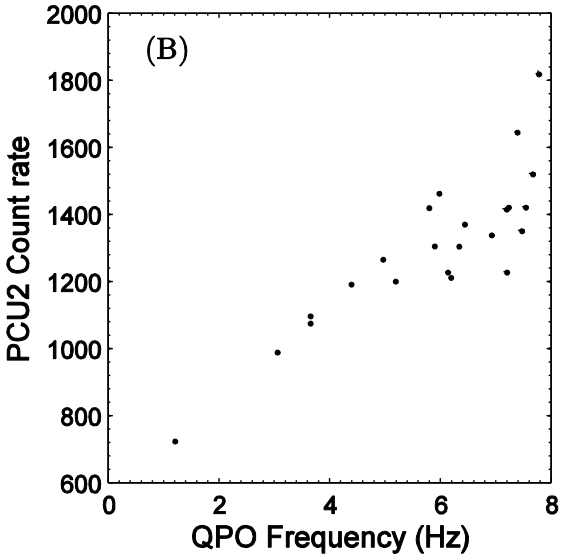

Flux and Hardness ratio are well correlated with QPO central Frequency.

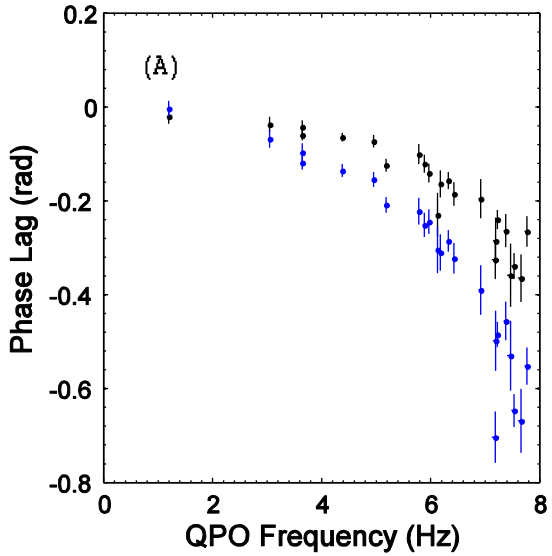

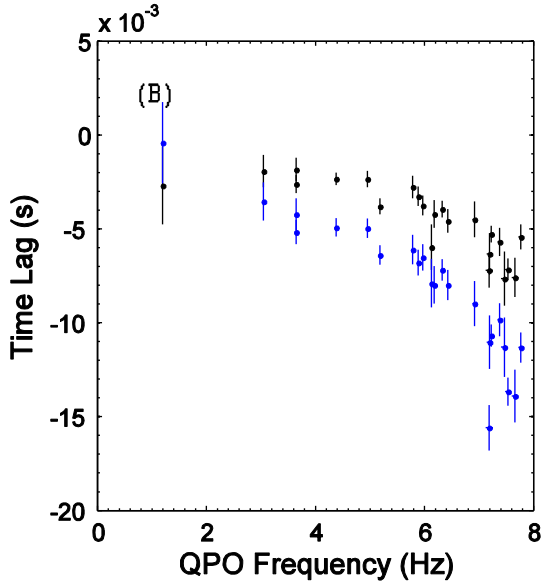

Contrary to XTE J1650-500，showing a increased soft lag with QPO frequency increasing.

XTE J1859+226 (Soft Delay)

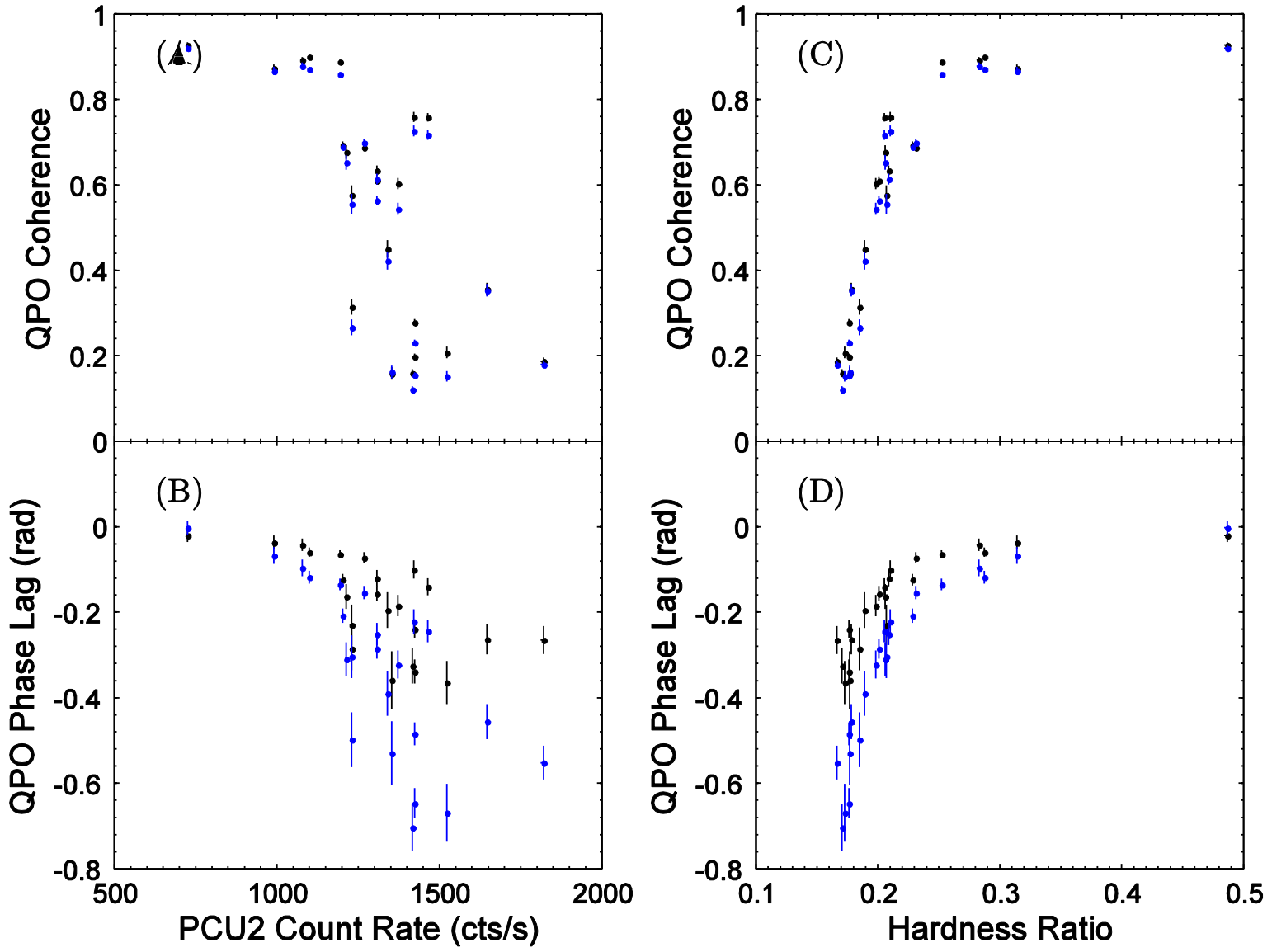

XTE J1550-564 (a special one)

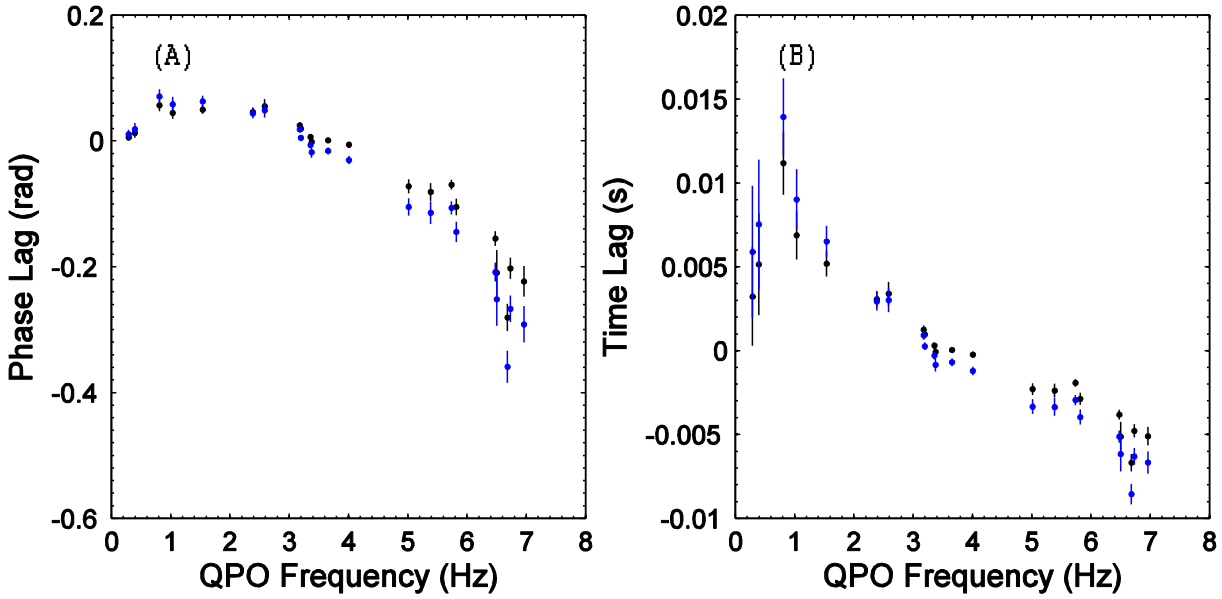

Outburst 1998

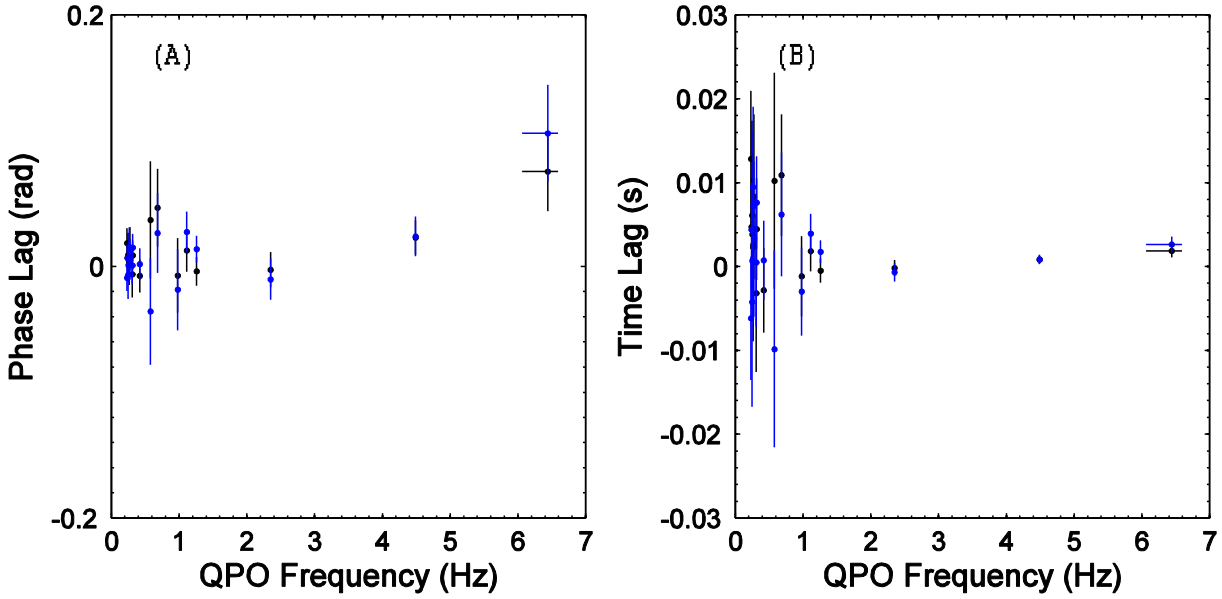

Outburst 2000

• Possible Classification

Inclination	transients	Outburst year	QPO (Hz)	Comments
Type-C Low Inclination	Swift J1753.5-0127	05, 10	0.37-0.90	Zero Delay
	4U 1543-47	02	4.3-11	Unknown
	XTE J1650-500	01	1.3-6.8	Hard Delay
	GX 339-4	02, 04, 07, 10	0.2-12	Hard Delay
	XTE J1752-223	09	2.2-6.4	Hard Delay
	XTE J1817-330	06	10-11	Unknown
Type-C Middle Inclination	XTE J1859+226	99	1.2-7.6	Soft Delay
	MAXI J1543-564	11	1.0-5.7	Zero Delay
Type-C High Inclination	XTE J1550-564	98, 00	0.1-13	A Special one
	4U 1630-47	02-04, 05	0.79-14.8	Unknown
	GRO J1655-40	96, 05	0.1-21	Zero Delay
	H 1743-322	03, 04, 08, 09, 10	0.11-9.44	Zero Delay
	MAXI J1659-152	10	1.6-7.3	Soft Delay
	XTE J1748-288	98	17-31	Unknown

SUMMARY

- Introduction to black-hole transients
- QPO and time lag models
- Research method
  - Three frequency ranges： Band-limited noise， Red noise and QPO
- The case of XTE J1650-500
  - Correlations and evolution
  - Fluctuation Propagation
- Preliminary results of other transients
  - Results and possible classification
  - Discussion